Received May 31, 2021, accepted June 21, 2021, date of publication July 13, 2021, date of current version July 21, 2021.

Digital Object Identifier 10.1109/ACCESS.2021.3096816

Experimental Study on Photodiode Array Sensor Aided MEMS Fine Steering Mirror Control for Laser Communication Platforms

FEMI ISHOLA AND MENGU CHO

Laboratory of Lean Satellite Enterprises and In-Orbit Experiments (LaSEINE), Kyushu Institute of Technology, Kitakyushu, Fukuoka 804-8550, Japan

Corresponding author: Femi Ishola (ishola.mustapha-femi741@mail.kyutech.jp)

ABSTRACT Line-of-sight laser communication application scenarios are numerous including land, mobile, maritime, airborne and space platforms for conventional and tactical utilization. However, beam pointing and stabilization are complicated in dynamic systems such as orbiting satellite to ground receiver, drones, aircrafts and metropolitan free-space optical links vulnerable to natural and artificial disturbances. Small Satellite platforms such as CubeSats are even more challenging due to their limited size and on-board resources. This paper presents an experimental study on a feedback photodiode array sensor assisted control of a one-axis micro-electromechanical (MEMS) fine steering mirror stabilizing a laser communication link on an optical bench in the laboratory. Disturbance profiles similar to vibrations on dynamic platforms are induced into the setup using an electrodynamic vibration machine to test the efficacy of the MEMS fine steering control mechanism. The Photodiode Array (PDA) sensor collocated with an Avalanche Photodiode at the receiving section provides sustained information about the transmitter's movements and beam displacements while the received optical signal strength is continuously monitored. The feedback signals are transmitted to the FSM controller via a radio link. We demonstrate the capacity to stabilize a laser beam transmission in the presence of external disturbances and platform movements using a PDA sensor assisted control.

INDEX TERMS Linear feedback control system, fine steering mirror (FSM), photodiode array sensor (PDA), platform vibrations.

I. INTRODUCTION

Since the advent of radio frequency (RF) communications in the early nineteenth century, it has been the mainstream mode of short and long distance connectivity but its capacity is now approaching the critical limits [1], [2]. The new era of big-data, internet of things (IoT) and growing information burst between multiple devices and platforms poses new challenges. The radio frequency spectrum is consistently congested while communication engineers and system architects usually have to work around signal interference problems especially in collocated and multi-node systems. On the contrary, the optical bands are underexplored, less regulated and without licensing complications. Optical communications have become very attractive alternative to RF for diverse applications because of its secured nature, larger channel bandwidth and extremely high data achievable rates. Eye safe infra-red lasers at moderate intensities are promising for next-generation ubiquitous metropolitan laser communication networks. Long range optical links are fast evolving from the expensive and cumbersome long-haul optical-fiber based systems to free-space optical transmissions (FSO). Compactness of the optical transceivers makes them to be easily hosted on diverse ground, maritime, airborne and space platforms as depicted in Fig.1 below. However, the suiting benefits of the narrow laser beamwidth simultaneously give rise to alignment challenges, pointing errors between the optical transmitter and receiver. Laser communications (Lasercom) are also vulnerable to weather conditions and atmospheric turbulence which attenuate, absorbs and scatter the signal during propagation [3].

High precision laser pointing, acquisition and tracking (PAT) mechanisms are indispensable in mitigating beam misalignment problems in optical links. PAT mechanisms are

The associate editor coordinating the review of this manuscript and approving it for publication was Qunbi Zhuge.

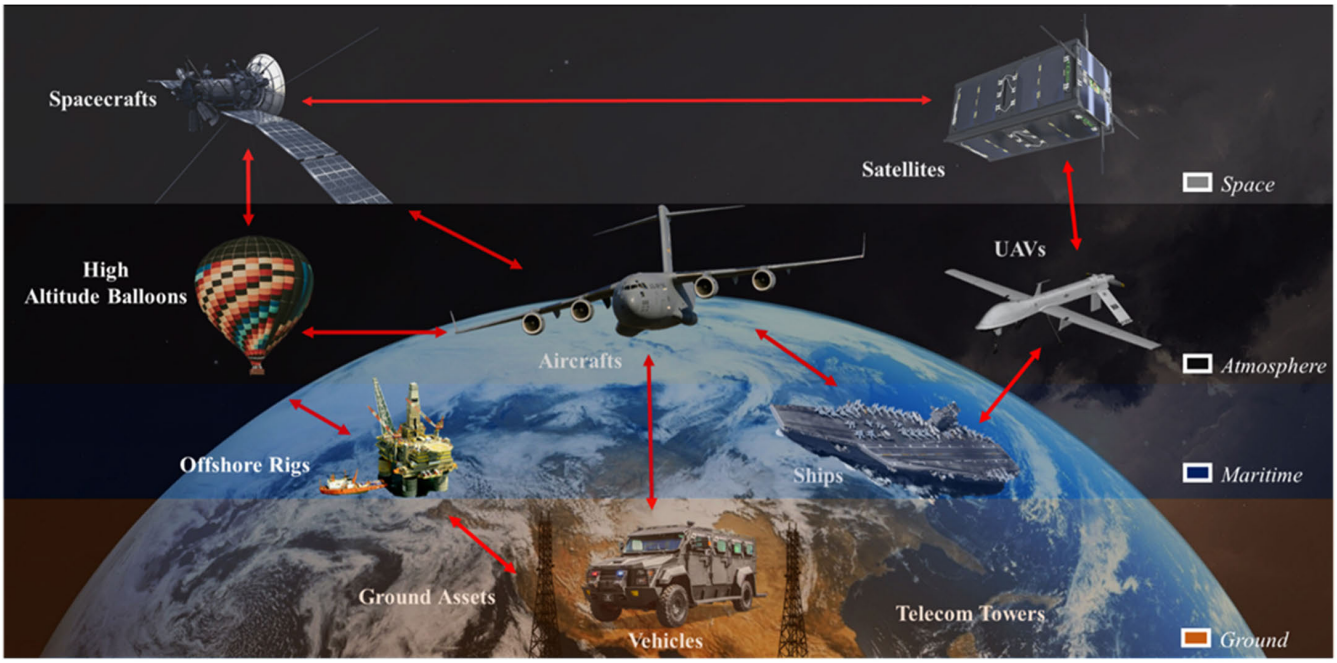

FIGURE 1. Dynamic and quasi-static laser communication scenarios.

generally implemented in two stages; coarse pointing and fine pointing subsystems for keeping the communication link [4]–[7]. Coarse pointing involves pre-aligning the optical heads, utilizing directional (guiding beacons) or positional sensors (GNSS) [8], attitude actuators and sometimes the platform's propulsion systems. Fine pointing systems (FPS) performs more accurate beam alignment and precision control irrespective of the platform's movement, attitude changes and induced jitter.

On satellite platforms, high-frequency micro-vibrations generated by the reaction wheel imbalances causes pointing instability [9], [10]. Rotary-wings based aircrafts and multi-rotor propelled drones also experiences significant vibrations that must be damped or isolated when hosting optical imaging or direct laser transmission devices [11]. Fine Steering Mirrors (FSM) are extensively used in laboratory optical setups and in lasercom FPS to maneuver outgoing laser beams to desired directions. Combination with inertia sensors such as accelerometers and gyroscopes enables continuous tracking of the platforms attitude and implementation of robust closed-loop control [12], [13]. Additional optical tracking Focal Plane Array (FPA) sensors such as Quadrant Detectors (QD), Position Sensitive Device (PSD) and Charge-Coupled Device (CCD Cameras) monitoring the transmitted beam enhances the performance of the FPS control system [14], [15]. CCD cameras are excellent choice for conducting detailed laser beam profiling but generally suffers low frame rate adding unwanted time delay to the control feedback loop and limiting the disturbance rejection bandwidth. They are also bulkier and consume more power than the others. PSDs are highly sensitive and provide rapid response [16]. QD and PSD are however limited in aperture size, often requiring the use of additional optics for wider field of view.

FPS for a low SWaP (size, weight and power), resource limited platform such as Cubesats and drones must be compact and efficient. A tradeoff consideration between key characteristics such as resolution, speed or sampling rate, effective aperture and power consumption of the most suitable optical tracking sensor becomes essential. In this paper, we introduce the use of an experimental auxiliary sensor; an 8 x 8 pixels photodiode array (PDA) to monitor the angular displacement of a transmitted laser beam and to support a fine laser pointing controller in the test system we constructed.

The purpose of the present paper is to report the performance of the photodiode array sensor as feedback device in the closed-loop control of a MEMS fine steering mirror reflecting a laser beam to a target position at the receiving side. The findings in this paper can benefit development of lightweight and robust fine pointing control systems for laser communication platforms. This paper is made up of five sections: the second and third parts describes the hardware and analyses of the test system respectively. Conducted laboratory experiments using the PDA assisted controller are presented in section four. The final part gives the conclusion and recommendations for future work.

II. DESCRIPTION OF BEAM STEERING TEST SYSTEM

A. TEST SYSTEM LAYOUT

The test apparatus illustrated in Fig. 2 consists of transmitting and receiving sections mechanically isolated from each other to emulate the case of distant laser communicating platforms as much as possible. The FSM and accelerometer sensors are collocated in order to track the attitude

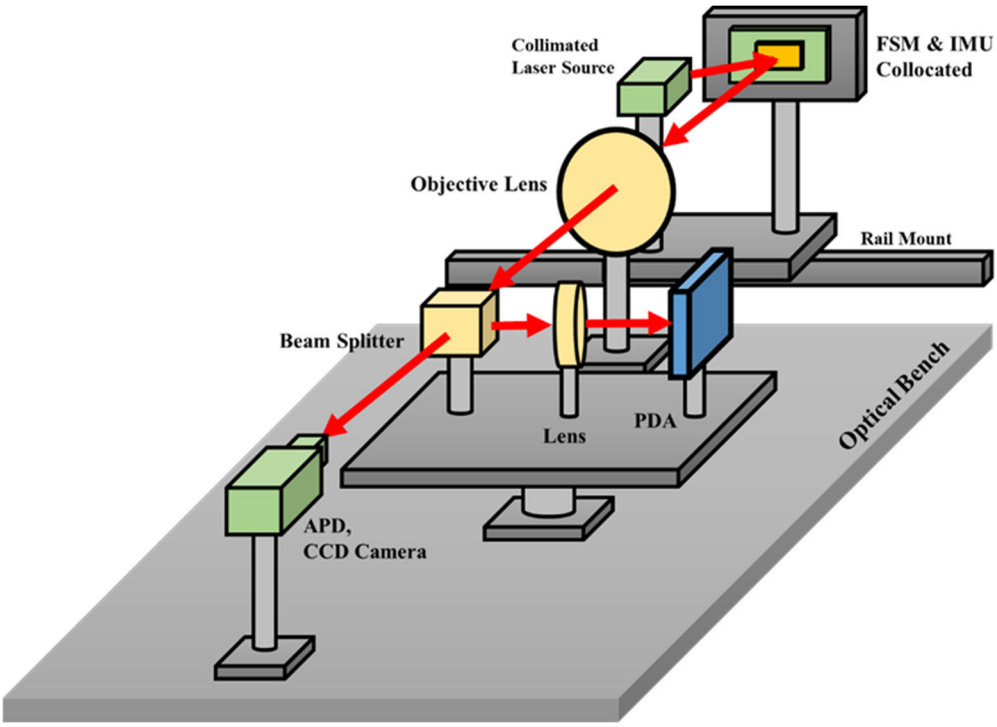

FIGURE 2. Layout of the beam steering test system.

changes of the transmitting platform and hence the beam due to induced vibrations. Both the optics and associated electronic circuitries are mounted on a rail for easy positional adjustments and coupling with the vibration generator. A mini-optical bench placed on top of an adjustable-height trolley host the receiving optics, thus enabling flexibility in aligning the systems. The sections were optically aligned such that in the absence of movements or disturbances, the receiving APD (ThorLabs' SM05PD3A) and the PDA sensor (Hamamatsu S13620-02) registers the maximum signal strength and zero angular beam displacement respectively. The APD was interchanged with a CCD Camera for profiling the beam characteristics.

B. TRANSMITTER AND BEAM CONTROLLER

A 1mW laser source with an in-built collimator generated Ø3 mm visible beam directed to the Hamamatsu S1227-03P MEMS Fine Steering Mirror. The laser diode was driven directly and also by an amplitude modulated circuit (not shown in Fig. 4) when transmitting test signals over the laser link. A low cost Commercial off-the-shelf (COTS) Arduino ATMega2560 microcontroller at the heart of the control circuitry receives feedback signals from an XBee radio link as well as continuous attitude data stream from MPU-6050 (3-axis Accelerometer and 3-axis Gyroscope) Inertia Measurement unit while executing the FSM control algorithm.

The Controller's digital voltage output (D_{nr}) was connected to MCP4725, a 12-bit resolution I2C digital-to-analog converter (DAC) and feedthrough to the Mirror driver

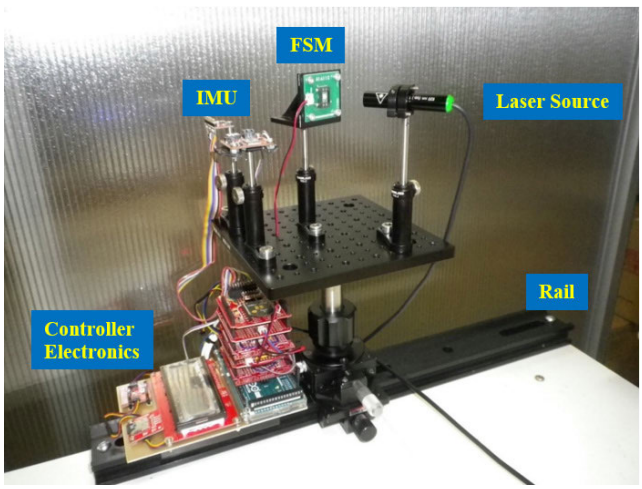

FIGURE 3. Prototype of the laser transmitter and FSM controller.

(LM324 quad-opamp voltage to current converter and monitor circuit). The Real time clock (RTC), LCD and datalogger also on I2C bus enables real-time visualization and recording of the system data during the vibration tests.

C. RECEIVING AND FEEDBACK SYSTEM

A Cubic Beamsplitter divides the received laser beam equally between the receiving APD/CCD Camera setup and the Photodiode Array Sensor system positioned 45° to each other on the optical bench. The beam's centroid and angular displacement across the aperture of the PDA is computed by

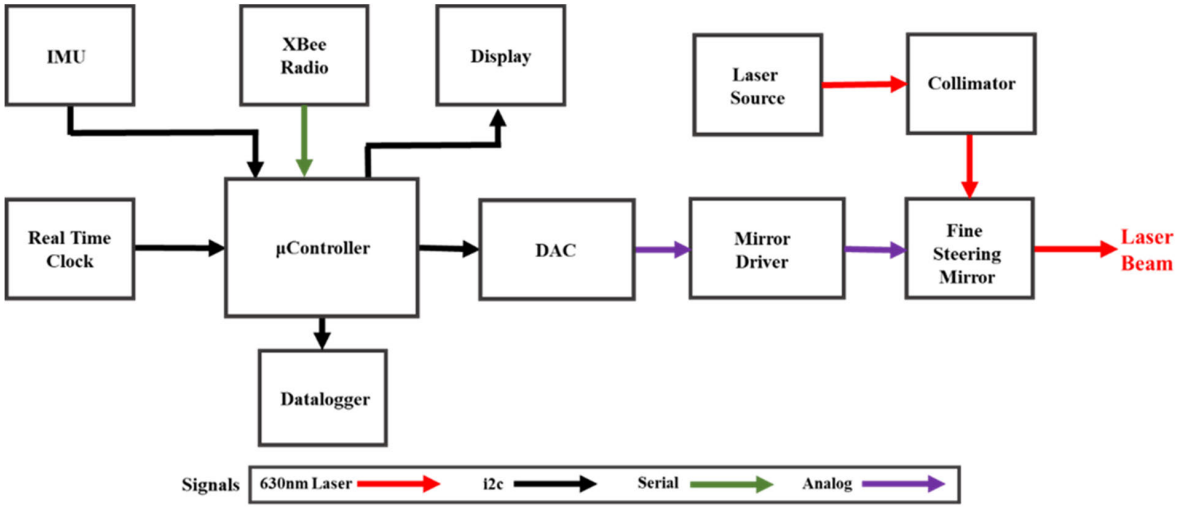

FIGURE 4. Block diagram of the transmitting section.

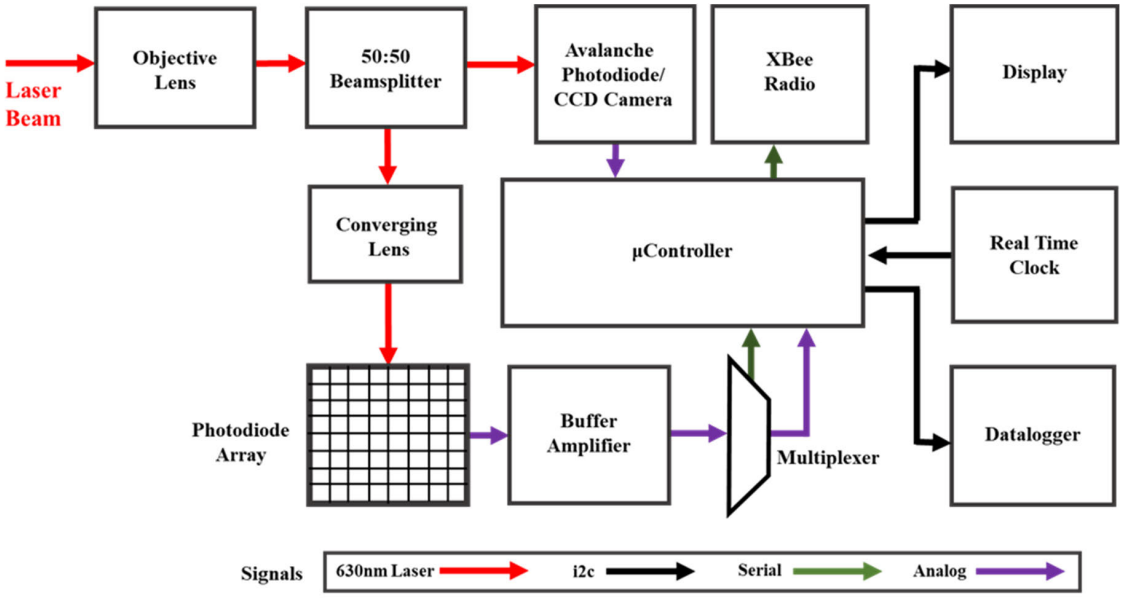

FIGURE 5. Block diagram of the receiving section.

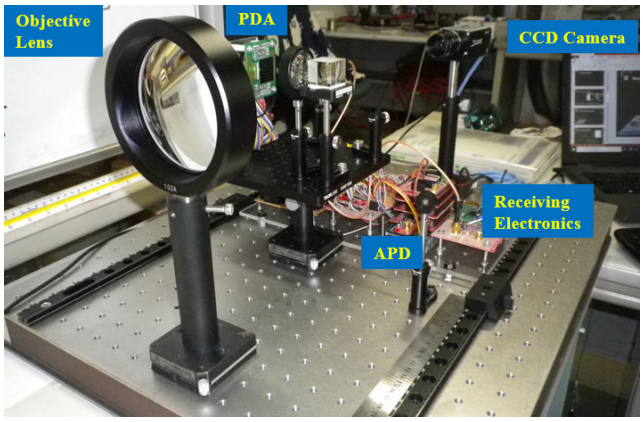

FIGURE 6. Prototype of the receiving section on an optical bench.

the microcontroller which then routes the information back to the transmitter's FSM controller via the XBee radio link. Similar to the transmitting section, a datalogger records the system information during the experiments. When a sufficient disturbance is applied to the transmitter platform, the beam position around the APD aperture fluctuates in proportion to the disturbance resulting to intermittent communication link outages. However, the PDA sensor continuously captures the angular deviation information needed for the FSM Controller to return the beam to the desired APD position.

D. PHOTODIODE ARRAY, BUFFER AND MULTIPLEXER

The PDA system comprises of the S13620-02 64-elements two dimensional array, 16 LTC1053 quad precision zero drift buffer amplifiers and 64-to-4 Multiplexer (CD74HC4067) circuit feeding four ADC channels of the microcontroller. The MCU clock speed and ADC sampling rate dictates the achievable frame rate of the PDA sensor system. ATMega2560 ADC

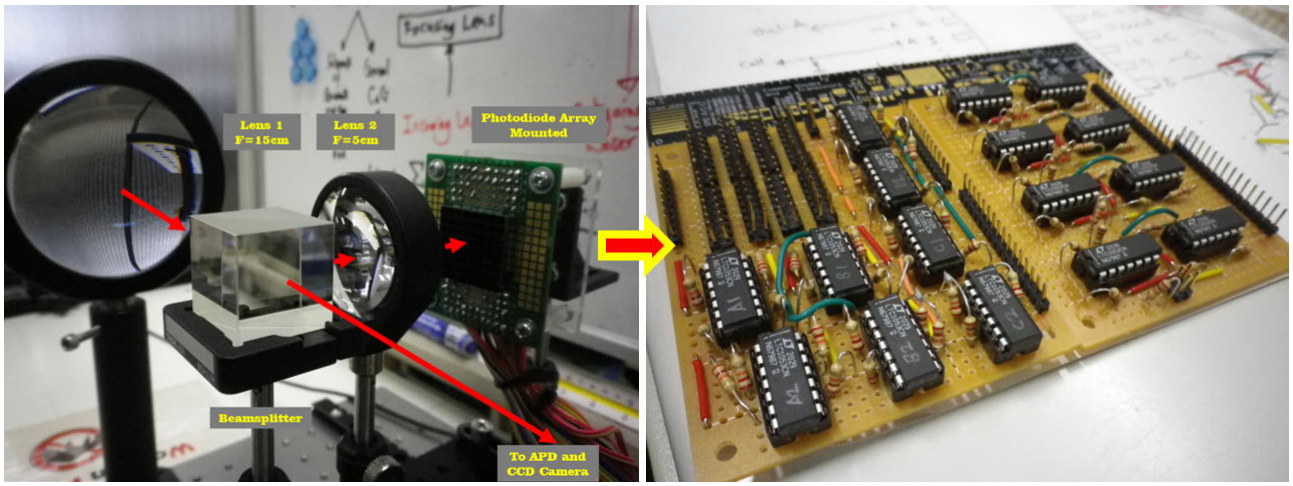

FIGURE 7. Receiver optics with mounted PDA and buffer-amplifier board.

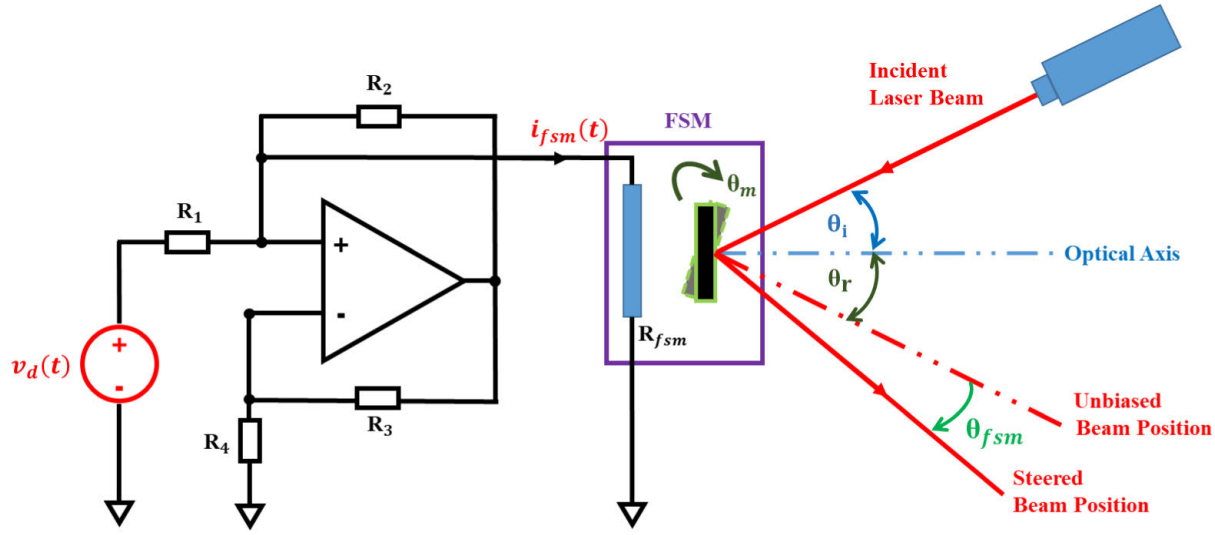

FIGURE 8. Operating principle of the MEMS FSM driver.

has 10 bit depth, with reliable sampled values when the ADC input clock is between 50 KHz and 200 KHz [17].

The MCU prescaler was adjusted to achieve 8MHz clock speed and with other program execution by the microcontroller, an actual frame rate of 50fps for the 64 pixels PDA was recorded. In comparison, the scA-1600 CCD Camera used in the experiment is capable of 14fps but 6 order of magnitude higher resolution than the PDA. Higher PDA frame rate is easily achievable by utilizing faster microprocessors and dedicated ADC chips such as 24-bits ADAS1127 delivering up to 20kSPS conversion rate. The PDA system frame rate must be sufficiently greater than (at least twice) the beam position fluctuation frequency in order to effectively track the beam and support the control system.

III. SYSTEM ANALYSIS

A. FSM FREQUENCY RESPONSE

The S12237-03P is an electromagnetic-type MEMS Fine Steering Mirror operated by applying a current source to its coil which has a typical resistance of 165Ω at room temperature. Because the coil resistance is susceptible to change due to the ambient temperature variations, a grounded load voltage to current converter ensures that actuation current is unaffected by these environmental changes. An upper limit of $\theta_{\text{fsm}} = 15°$ optical deflection angle and 100Hz drive frequency was recommended by the device manufacturer [18]. Therefore, R1 to R4 = 333.3Ω was adopted for V_{dd} =5V DAC reference. The maximum drive frequency sets the bandwidth of the platform disturbance rejection.

$$V_d\,(t) = v_{dd}\frac{D_{nr}}{(2^n-1)}; n = 12bits \tag{1}$$

$$i_{fsm}\,(t) = \frac{v_d\,(t)}{R_1} \tag{2}$$

The FSM optical deflection angle is always twice the mechanical angle, θ_{m} with good linearity when driven

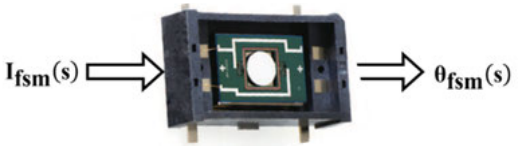

FIGURE 9. FSM transfer function.

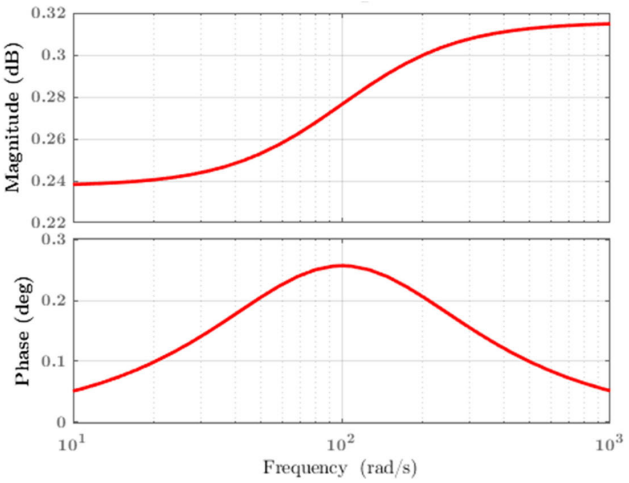

FIGURE 10. FSM open-loop frequency response.

between -15mA to 15mA as expressed in (3).

$$\theta_{fsm}(t) = 2\theta_m = i_{fsm}(t) \times 1000 \tag{3}$$

Equation (4)-(7) is the Plant (FSM) transfer function with its complex response; amplitude and phase lag expressed as a function of the drive frequency, resonant frequency (530Hz) and the device Quality factor, Q = 30.

$$G_{fsm}(s) = \frac{I_{fsm}(s)}{\theta_{fsm}(s)} \tag{4}$$

$$G_{fsm}(\omega) = \left|G_{fsm}(\omega)\right| e^{arg\{G(\omega)\}} \tag{5}$$

$$\left|G_{fsm}(\omega)\right| = 1 + \left(\frac{\omega}{530}\right)^2 \tag{6}$$

$$arg\{G(\omega)\} = tan^{-1}\left\{\frac{530\omega}{Q\left(280900 - \omega^2\right)}\right\} \tag{7}$$

MATLAB System Identification Toolbox was utilized to obtain the Plant's poles-zero gain mathematical model:

$$G_{fsm}(s) = \frac{1.037S + 103.8}{S + 101} \tag{8}$$

B. PDA BEAM CENTROID

The 8 x 8 elements resolution array was selected as the primary sensor for optical feedback in the experiment because higher frame rates can be achieved compared to CCD cameras, effectively trading resolution for faster response speed. However, elemental pixel gaps or dead zones in the array impacts the overall precision of the PDA. The received laser beam at the PDA surface has a Gaussian distribution with ~3mm spot size comparable to the width of each pixel $l_q = 3mm$. Bisection of the beam's intensity is concentrated within the Full Width at Half Maximum (FWHM),

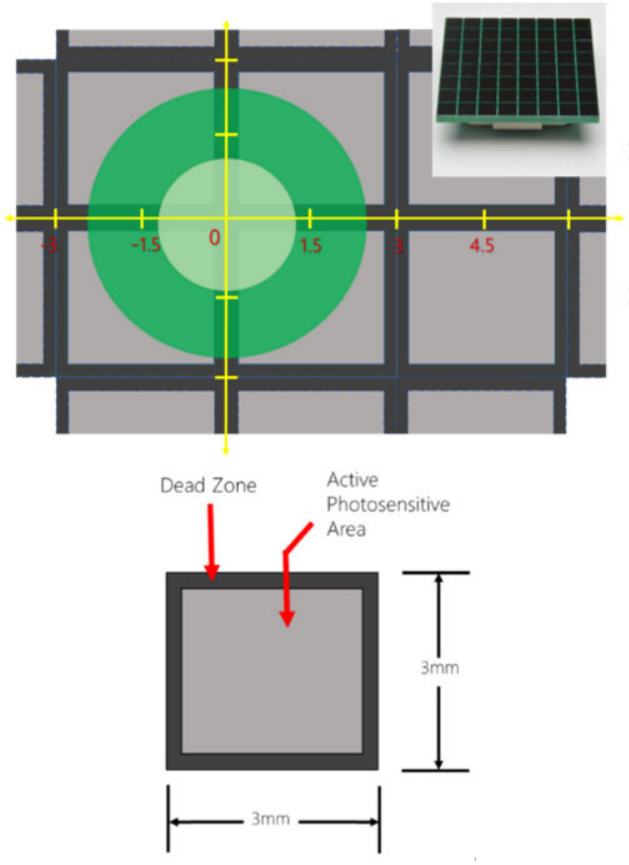

FIGURE 11. Scaling of the PDA aperture and pixel size (Inset: Hamamatsu S13620-02).

hence centroid calculation was simply implemented using the Center-of-Gravity (CoG) algorithm expressed in (9), having the benefit of lower computing power requirement [19].

$$(x, y) = 4l_q\left\{\frac{\sum X_{ij}I_{ij}}{\sum I_{ij}}, \frac{\sum Y_{ij}I_{ij}}{\sum I_{ij}}\right\} \tag{9}$$

Quadrant Detectors (2 × 2 array) and Position Sensitive Devices (PSD) are commonly used for laser beam displacement measurement but have limited aperture size making them unfitting for sensing larger angular displacements without the use of additional optics. Beam centroid using QDs are done by continuous sampling of the currents from the four photodiode's quadrants as in (10). The PDA can also be modeled as a stack of multiple QDs to enable wider aperture sensing.

$$(\Delta x, \Delta y) = 4\left(l_q\left\{\frac{(I_A + I_D) - (I_B + I_C)}{I_A + I_B + I_C + I_D}\right\}, l_q\left\{\frac{(I_A + I_B) - (I_C + I_D)}{I_A + I_B + I_C + I_D}\right\}\right) \tag{10}$$

C. FEEDBACK CONTROLLER

A Proportional-Integral (PI) Controller was designed in Simulink to drive the FSM in single-loop (i.e. using only PDA feedback). Optimal values of the control gains Kp, Ki were designed in Simulink for a stable control system

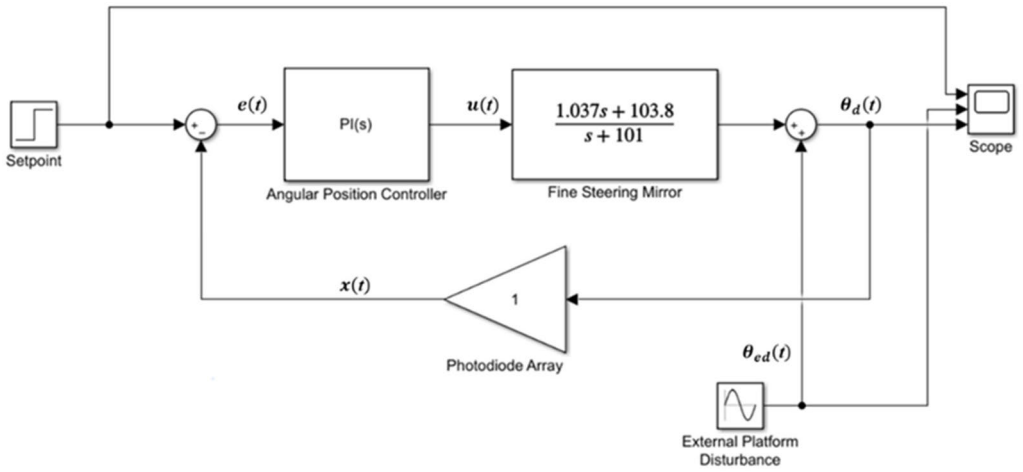

FIGURE 12. PDA single-loop feedback control model.

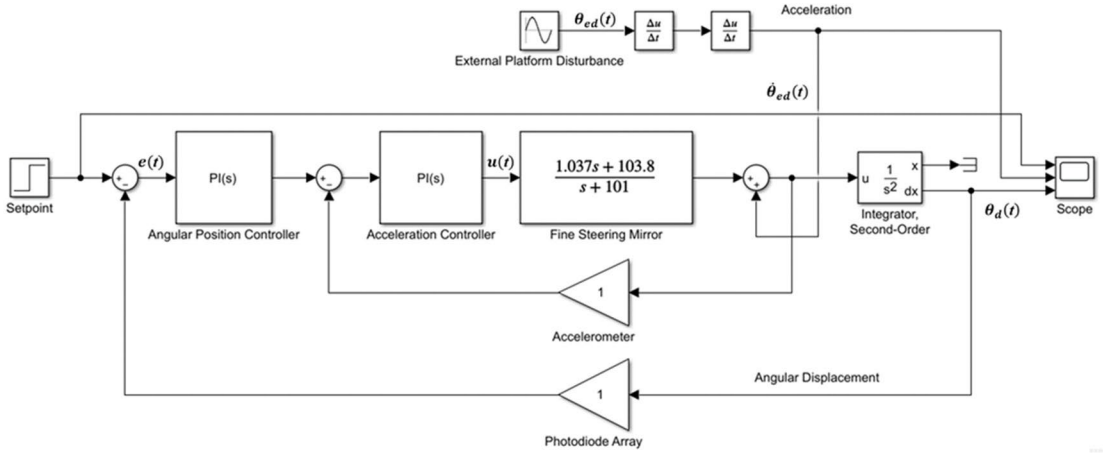

FIGURE 13. PDA and accelerometer double-loop feedback model.

with no overshoot and minimal rise time (5ms) to achieve close-loop bandwidth of 100Hz. The MPU6050 device gyroscope and accelerometer maximum bandwidths are specified as 8 KHz and 1 KHz respectively [20]. In double-loop control mode, featuring the PDA and accelerometer feedbacks, the accelerometer is positioned in the inner loop because of its high bandwidth. In the actual experiment, the platform was subjected to vibrations at different linear acceleration and displacement values for only the single mode. Fig.14 shows the simulated response to a sinusoidal external vibration with a sinusoidal profile of 4 degrees amplitude and 5 Hz frequency with 0.5s step time of the SetPoint.

The controller output oscillates by about the same frequency but its amplitude constrained to the SetPoint value (expected beam position) which is adequate to keep the laser communication link within the APD's field-of-view. Driving the FSM at values closer to its mechanical resonant frequency produces severe inaccuracies and instability because the optical deflection angular error and phase lag increases with Controller's output frequency. The Hamamatsu S12237-03P

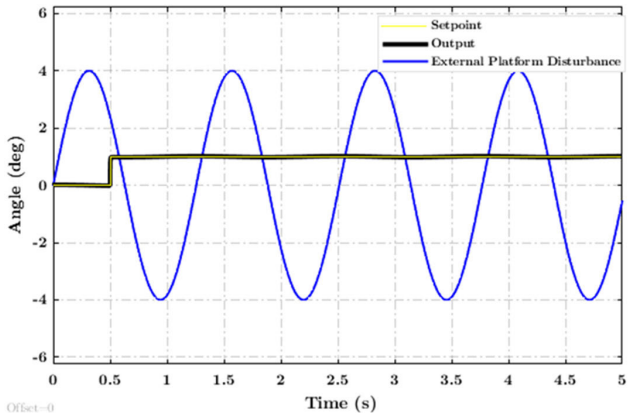

FIGURE 14. Simulated controller response to unit-step setpoint and sinusoidal disturbance profile.

FSM can be reliably operated at 100Hz in linear mode, hence setting a limit for the system's vibration disturbance bandwidth. The choice of FSM is therefore based on the prior knowledge of the expected platform jitter bandwidth and sampling rates of the feedback sensors.

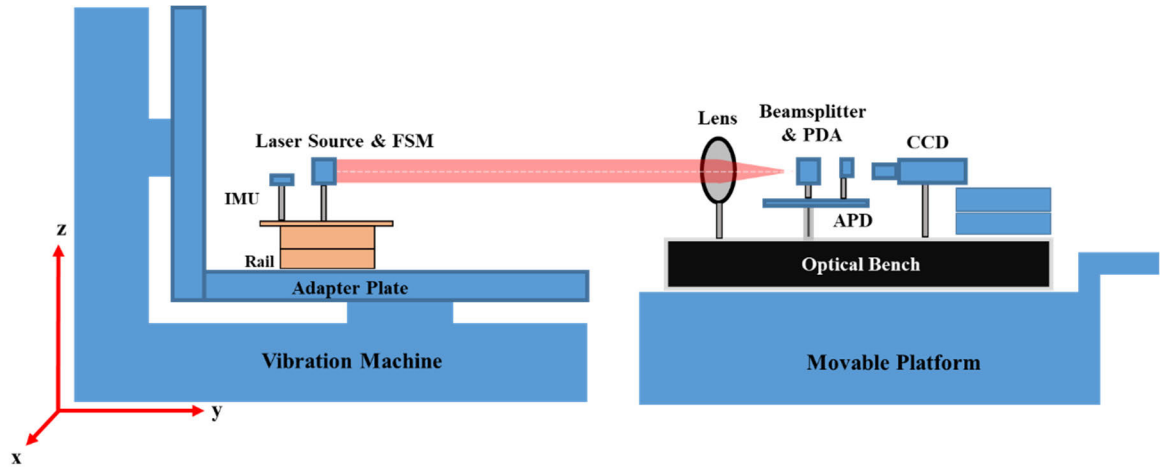

FIGURE 15. Layout of vibration machine test setup.

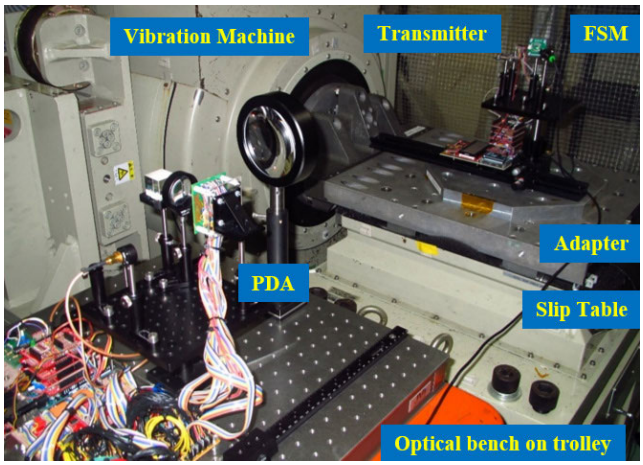

FIGURE 16. Vibration testing machine integration.

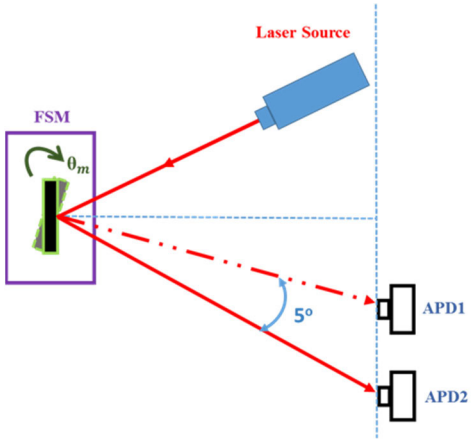

FIGURE 17. APDs setup.

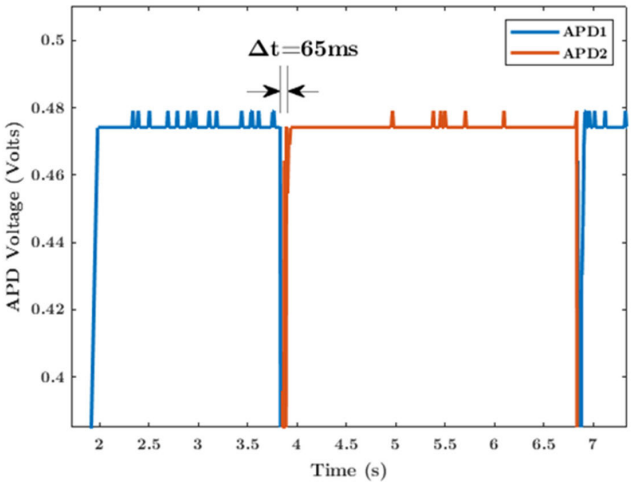

FIGURE 18. Beam switching response.

IV. EXPERIMENTAL VALIDATION AND RESULTS

A. METHODOLOGY

The objective of the beam steering experiment was to test the performance of the FSM feedback Controller utilizing the PDA in suppressing the induced platform disturbances at varying vibration profiles. The transmitter setup consisting of the laser source, FSM, inertia sensor and Controller were firmly assembled on a mini-optical breadboard attached to a rail. The rail was firmly attached to an adapter jig on top of the vibration machine's slip table. The vibration machine is an industrial grade test system used for satellite qualification tests at the Kyushu Institute of Technology's Center for Nanosatellite Testing. The machine is capable of generating vibrations of up to 2 KHz frequency and 10cm linear displacement covering most of satellite launch and on-orbit jitter spectrum. The receiving and feedback system were assembled on a small optical bench placed on a moveable trolley. At first, the platforms were arranged such that the laser beam was perfectly aligned with the axis of the PDA and APD sensors. Therefore the position of the platforms were fixed while only the vibration machine altered the attitude of the stabilized transmitting setup in the x-axis direction as shown above. The two sections were completely mechanically isolated, the XBee radio feedback link also eliminated the need for cabling between them. During the vibration experiment, the transmitter platform was subjected to different acceleration movements to check the PDA feedback alignment error and FSM Controller responses.

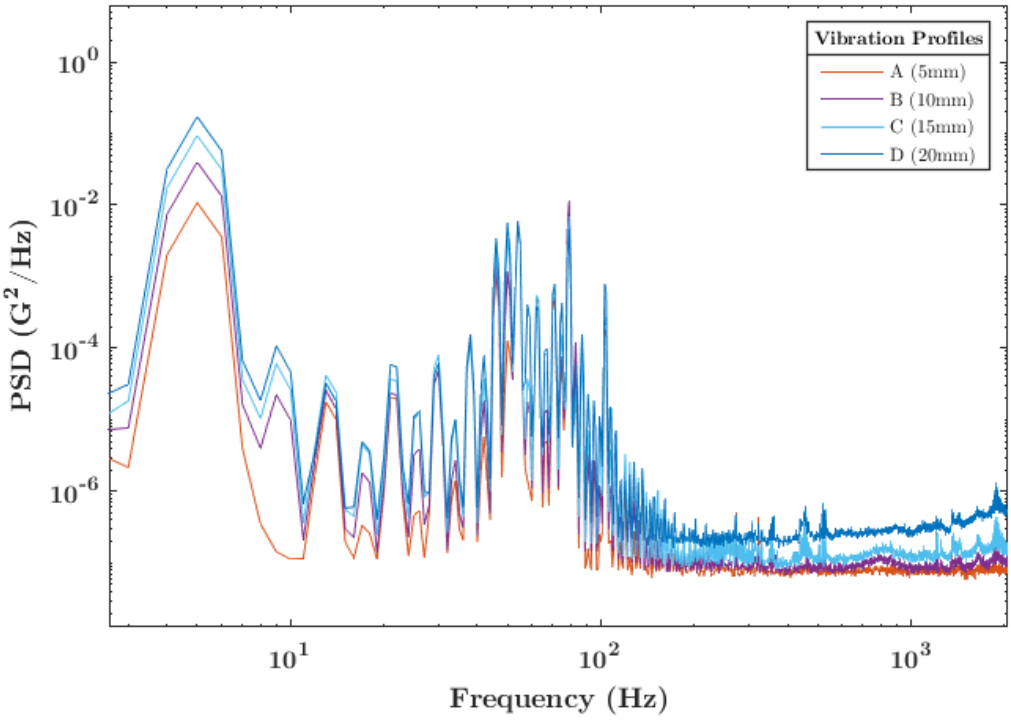

FIGURE 19. Frequency spectrum of vibration machine profiles at FSM and Accelerometer position.

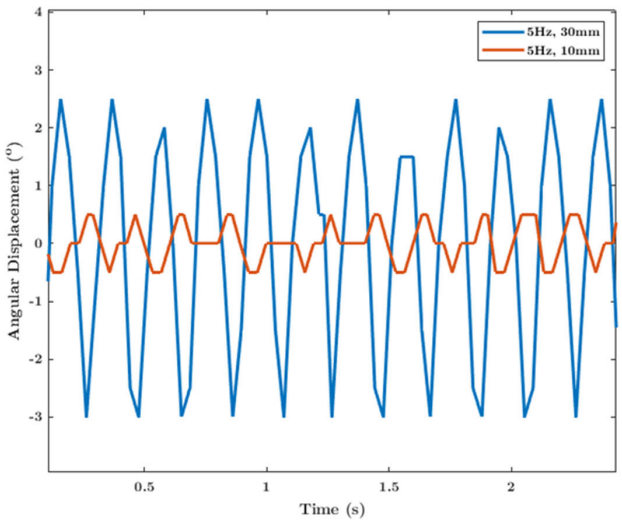

FIGURE 20. Open loop response to vibration machine disturbances.

B. FSM BEAM SWITCHING BETWEEN TWO APDs

Prior to coupling of the test system to the vibration machine, an open-loop laser switching between two APDs separated at a known beam angular displacement (5°) to check the accuracy of the fine steering mirror. The Controller was programmed to retain the beam at APD1 and APD2 positions for 2s and 3s respectively. Fig. 18 shows the raw sampled ADC readings of the APDs in response to the beam movements. The spikes in the curves represents the background noise at the aperture of the detectors. The test established the accuracy of the FSM.

TABLE 1. Experiment vibration test profiles.

Vibration Machine Profiles	*Acceleration (G)*	*Set Mean Frequency (Hz)*	*Linear Displacement Amplitude (mm)*
Profile A	0.25	5.00	5.00
Profile B	0.50	5.00	10.00
Profile C	0.75	5.00	15.00
Profile D	1.00	5.00	20.00

C. VIBRATION MACHINE DISTURBANCES TEST PROFILES

In the closed-loop control operation, the transmitter system was subjected to four vibration profiles with characteristics provided in the table below. The vibration machine was programmed to move the slip table at 5Hz sinusoidal pattern at different amplitudes. However, the actual nature of vibrations at the sensor locations close to the FSM contains multiple frequencies and harmonics due to the mechanical parts of the laser transmitter. Therefore the PSD plot in Fig. 19 shows the actual vibration pattern obtained at the FSM position.

D. OPEN LOOP PDA RESPONSE TO BEAM DISTURBANCES

The vibration machine was operated at different frequencies and displacements without activating the FSM Controller and the radio feedback signal. This enabled the assessment of the PDA response to the beam disturbance profiles. As shown in Fig. 20, the angular deviation oscillate in consonance with the vibration machine profiles.

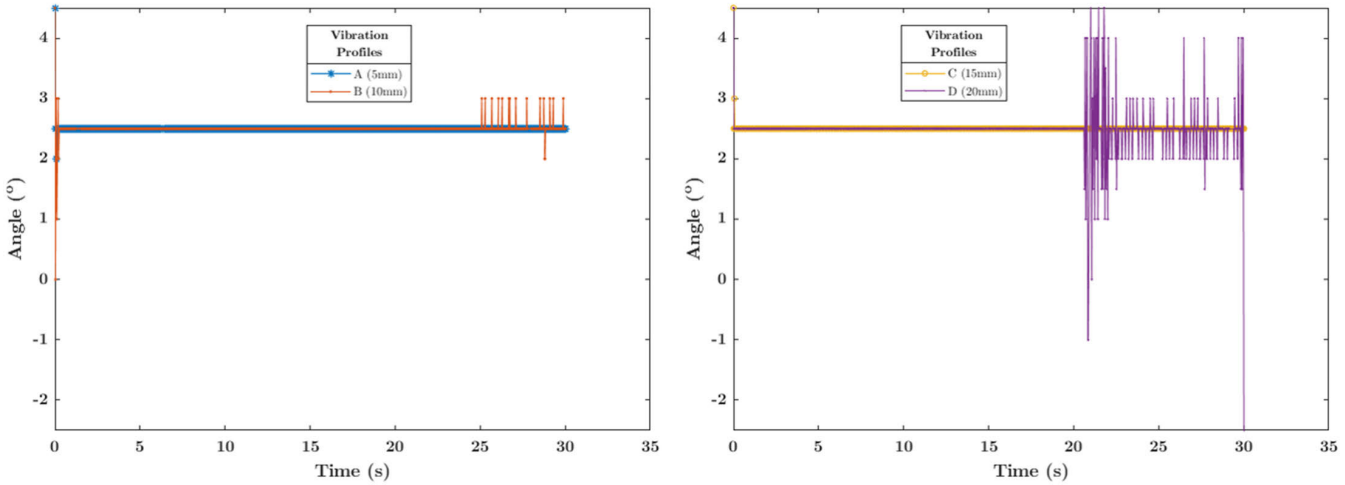

FIGURE 21. Closed loop beam stabilization under vibration machine disturbances.

E. CLOSED LOOP BEAM STABILIZATION UNDER VIBRATION MACHINE DISTURBANCES

In the closed-loop mode, the beam angular displacement values computed using the PDA sensor was relayed to the Controller at the transmitter. Therefore the FSM was constantly actuated automatically to suppress the vibration profiles by deflecting the beam to the desired angular setpoint (2.5°). Fig. 21 shows the PDA response and the feedback controller effort.

The Controller steered the beam adequately in the Profiles A, B and C but was less effective in Profile D due to the larger displacement of the slip table, microcontroller performance and the XBee feedback channel. The overlapping flat lines in the plots shows that the laser beam was stabilized for over 20 seconds despite the induced fluctuations by the vibration machine. In these periods the PDA circuitry sends back continuous streams of beam angular error to the FSM controller. This demonstrated that a lower resolution PDA sensor can effectively substitute CCD cameras in feedback beam control for low resource platforms.

V. CONCLUSION

MEMS Fine Steering Mirrors are critical actuators in lasercom fine beam pointing and platform disturbance suppression systems because they are miniature, easy to drive, agile and demand less platform resources. They are often combined with optical sensors such as quad cells (QD), position sensitive devices (PSD) and CCD cameras in close-loop automatic control of the beam position. CCD cameras has slow detection and processing speeds while the field-of-regard is very limited in QDs and PSDs due to their smaller aperture size. In QDs, the laser beam spot size after focusing usually are comparable to the quadrant pixel size hence restricting the beam deviation on the surface to limited amounts.

We have introduced the use of scalable photodiode array as the optical feedback sensor for fine beam pointing and control. We demonstrated by experiment using COTS components that a photodiode array with a much lower resolution compared to CCD camera but having faster response can assist a close-loop fine beam position control. The spatial size of the PDA sensor can be increased if desired depending on the specific application requirements. Much higher detection frame rates are also achievable with increased computing capacity by using faster microprocessors. The PDA sensor is attractive for use on resource-limited platforms such as small satellites, CubeSats, unmanned aerial vehicles and high altitude vehicles where size, weight, and power supply are tightly managed and distributed.

Combination with tunable spectral filters makes the PDA a very unique sensor capable of detecting multiple wavelength lasers position in a single package. This comes with enormous advantages in applications such as densed wavelength division multiplex systems (DWDM) and bi-directional optical communication modules that utilizes many laser beams for uplink and downlink, drastically reducing the number of optics, weight and power consumption.

Future work will address minimizing effects of the narrow elemental gaps and dead zones on the precision of dynamic laser beam centroid computation. More efficient centroiding algorithms such as the best-fit to Gaussian approach will enhance the detection accuracy of the photodiode array sensor and consequently the performance of the fine steering control system.

REFERENCES

[1] Y. Karasawa, "On physical limit of wireless digital transmission from radio wave propagation perspective: Physical limit of wireless transmission," *Radio Sci.*, vol. 51, no. 9, pp. 1600–1612, Sep. 2016, doi: 10.1002/2016RS006040.

[2] C. E. Shannon, "A mathematical theory of communication," *Bell Syst. Tech. J.*, vol. 27, no. 3, pp. 379–423, Jul. 1948, doi: 10.1002/j.1538-7305.1948.tb01338.x.

[3] Y. Kaymak, R. Rojas-Cessa, J. Feng, N. Ansari, M. Zhou, and T. Zhang, "A survey on acquisition, tracking, and pointing mechanisms for mobile free-space optical communications," *IEEE Commun. Surveys Tuts.*, vol. 20, no. 2, pp. 1104–1123, 2nd Quart., 2018, doi: 10.1109/COMST.2018.2804323.

[4] C. Schmidt and J. Horwath, "Wide-field-of-regard pointing, acquisition and tracking-system for small laser communication terminals," in *Proc. ICSOS*, 2012, p. 6.
[5] P. W. Young, L. M. Germann, and R. Nelson, "Pointing, acquisition, and tracking subsystem for space-based laser communications," *Proc. SPIE*, vol. 0616, pp. 118–128, May 1986, doi: 10.1117/12.961045.
[6] P. Grenfell, A. Aguilar, K. Cahoy, and M. Long, "Pointing, acquisition, and tracking for small satellite laser communications," in *Proc. Small Satell. Conf.*, Aug. 2018. [Online]. Available: https://digitalcommons.usu.edu/smallsat/2018/all2018/418
[7] J. Chang, C. M. Schieler, K. M. Riesing, J. W. Burnside, K. Aquino, and B. S. Robinson, "Body pointing, acquisition and tracking for small satellite laser communication," *Proc. SPIE*, vol. 10910, Mar. 2019, Art. no. 109100P, doi: 10.1117/12.2511159.
[8] B. Epple, "Using a GPS-aided inertial system for coarse-pointing of free-space optical communication terminals," *Proc. SPIE*, vol. 6304, Sep. 2006, Art. no. 630418, doi: 10.1117/12.680502.
[9] L. Li, L. Yuan, L. Wang, R. Zheng, Y. Wu, and X. Wang, "Recent advances in precision measurement & pointing control of spacecraft," *Chin. J. Aeronaut.*, Jan. 2021, doi: 10.1016/j.cja.2020.11.018.
[10] C. J. Dennehy, "A survey of reaction wheel disturbance modeling approaches for spacecraft line-of-sight jitter performance analysis," in *Proc. Eur. Space Mech. Tribol. Symp.*, Sep. 2019, p. 13.
[11] W. H. Semke and M. D. Dunlevy, "A review of the vibration environment onboard small unmanned aircraft," in *Sensors and Instrumentation, Aircraft/Aerospace and Energy Harvesting*, vol. 8. Cham, Switzerland: Springer, 2019, pp. 155–164, doi: 10.1007/978-3-319-74642-5_18.
[12] J. Tian, W. Yang, Z. Peng, T. Tang, and Z. Li, "Application of MEMS accelerometers and gyroscopes in fast steering mirror control systems," *Sensors*, vol. 16, no. 4, p. 440, 2016, doi: 10.3390/s16040440.
[13] H. Zhang, Y. Mao, J. Deng, and H. Liu, "Three closed-loop feedback control system with dual disturbance observers of an optoelectronic stable control platform," *Electronics*, vol. 9, no. 2, p. 359, Feb. 2020, doi: 10.3390/electronics9020359.
[14] J. Sofka, V. V. Nikulin, V. A. Skormin, D. H. Hughes, and D. J. Legare, "Laser communication between mobile platforms," *IEEE Trans. Aerosp. Electron. Syst.*, vol. 45, no. 1, pp. 336–346, Jan. 2009, doi: 10.1109/TAES.2009.4805283.
[15] C. Deng, Y. Mao, and G. Ren, "MEMS inertial sensors-based multi-loop control enhanced by disturbance observation and compensation for fast steering mirror system," *Sensors*, vol. 16, no. 11, p. 1920, Nov. 2016, doi: 10.3390/s16111920.
[16] B. Hou, "Charge-coupled devices combined with centroid algorithm for laser beam deviation measurements compared to a position-sensitive device," *Opt. Eng.*, vol. 50, no. 3, Mar. 2011, Art. no. 033603, doi: 10.1117/1.3554379.
[17] *Atmel-2560 Datasheet*. Accessed: Feb. 22, 2021. [Online]. Available: https://ww1.microchip.com/downloads/en/devicedoc/atmel-2549-8-bit-avr-microcontroller-atmega640-1280-1281-2560-2561_datasheet.pdf
[18] *S12237-03 Datasheet*. Accessed: Feb. 22, 2021. [Online]. Available: https://www.hamamatsu.com/resources/pdf/ssd/s12237-03p_koth1006e.pdf
[19] A. Vyas, M. B. Roopashree, B. R. Prasad, and A. Vyas, "Performance of centroiding algorithms at low light level conditions in adaptive optics," in *Proc. Int. Conf. Adv. Recent Technol. Commun. Comput.*, Kottayam, India, Oct. 2009, pp. 366–369, doi: 10.1109/ARTCom.2009.30.
[20] *MPU6050 Datasheet*. Accessed: Feb. 22, 2021. [Online]. Available:https://cdn.sparkfun.com/datasheets/Components/General%20IC/PS-MPU-6000A.pdf

FEMI ISHOLA received the B.S. degree in electrical/electronics engineering from the University of Lagos, Nigeria, in 2010, and the M.S. degree from the International Space University, France, in 2014. He is currently pursuing the Ph.D. degree with the Laboratory of Lean Satellites Enterprises and In-Orbit Experiments, Kyushu Institute of Technology, Japan. His Ph.D. research is focused on deep space optical communication technologies for small satellites. He is currently a Research Assistant with the Laboratory of Lean Satellites Enterprises and In-Orbit Experiments, Kyushu Institute of Technology, and a Visiting Collaborative Researcher with the Space Communications Laboratory, National Institute of Information Communications Technology (NICT), Tokyo, Japan. He participated in the Southern Australian Universities QB50 Collaboration Satellite project. He was the Pioneer and a Project Manager of the CSTP Ground Control Station. He was a recipient of the Kano State Government Award for the Best Millennium Development Goals (MDGs) Project, in 2011, and the International Astronautical Federation (IAF) Emerging Space Leaders Grant Award, in 2019.

MENGU CHO received the B.S. and M.S. degrees from The University of Tokyo, and the Ph.D. degree from the Massachusetts Institute of Technology, in 1992. After working at Kobe University and International Space University, he joined the Kyushu Institute of Technology (Kyutech), in 1996. Since 2004, he has been a Professor. He is currently the Director of the Laboratory of Lean Satellite Enterprises and In-Orbit Experiments. He has supervised 11 university satellite projects, among which nine projects, 19 satellites, were already launched. He has authored or coauthored more than 180 articles in peer-reviewed journals. His research interests include spacecraft environmental interaction, satellite systems, and nano-/micro-satellite development and applications. In 2019, he received the Frank J. Malina Astronautics Medal from International Astronautical Federation.